

EVLA Memo No. 87

Design, Prototyping and Measurement of EVLA L-Band Feed Horn

Sivasankaran Srikanth, Jim Ruff and Ed Szpindor
NRAO

March 22, 2005

Abstract:

A wideband, compact, corrugated feed horn for L-band (1-2 GHz) has been designed, built and tested. The feed has average illumination tapers of -9.6 dB from 1.0-2.0 GHz and -10.3 dB from 1.2-2.0 GHz. Cross-polarization is < -27.0 dB over the entire frequency band. Measured return loss is -16 dB at 1.0 GHz and better than -20 dB above 1.03 GHz. Calculated aperture efficiency on the VLA antenna is 0.45 at 1.4 GHz and 0.54 at 2.0 GHz.

Introduction:

One of the goals of the VLA Expansion (EVLA – Phase 1) Project is to provide continuous frequency coverage with increased sensitivity from 1 to 50 GHz from the secondary focus. A new feed cone has been designed to accommodate the eight secondary focus feeds and receivers covering the above frequency range. With the exception of the K- and Q-bands, the other six bands will have new receivers and feeds. The design of the L-band feed with an octave bandwidth (1–2 GHz) was critical as its size dictated the layout of the feeds on the feed cone. A gain/system temperature (G/T) analysis was done at L-band in order to determine the optimum taper for the feed. G/T peaked at -17 dB feed taper for a receiver temperature of 13 K. A compact horn with a -13 dB taper at the edge of the subreflector (9.3°) will have an outside diameter (OD) of 93" at the aperture and will be 263" long. The space available on the feed cone allowed a maximum OD of 75" for the L-band feed horn. However, a feed with an OD of 75" was still too long and would have required structural modification to the VLA antenna. By scaling this feed by a factor of 1.2:1, the OD became 63" and the length 165". The average tapers in the 1-2 GHz range for the 75" and 63" feeds are -10.0 and -9.3 dB, respectively. Performances of the VLA antenna with the 63" compact horn and the VLA L-band hybrid feed are compared at different elevation angles in Figures 1 and 2. The VLA feed has a higher G/T over a small frequency range, compared to the new design, at elevation angles of 60° and higher. Below 60° elevation of the VLA antenna, the new design has a superior G/T performance. In this memo, details of the design of the feed, measurements on the scaled prototype, and measurements on the L-band prototype are presented.

Design:

The type of feed selected for the L-band is a compact or profile horn [1], [2]. In this type of horn, the transition from the throat to the aperture has a cosine taper in place of a linear taper. This reduces the length of the horn by about 30% when compared to a linear taper horn for a given illumination taper. In addition, the aperture of the horn is smaller by about 20%. In the L-band design, the mode converter, where the TE_{11} mode of the circular waveguide is converted to the hybrid HE_{11} mode, has a linear taper of 8° . Ring-loaded corrugations [3] with constant depth are used in the mode converter section for obtaining the wide bandwidth. The diameter at the first corrugation is 7.5" in order to avoid generation of the EH_{12} mode. The input of the feed also has a diameter of 7.5" and a transition 10" long connects the input section to the mode converter. The number of corrugations per wavelength at 2.0 GHz was chosen to be about 4 in order to keep the manufacturing cost low. The pitch is 1.575", and the flange thickness is 0.090". There are seven ring-loaded corrugations, formed from machined aluminum disks, in the mode converter. These disks are positioned inside a bore in a machined housing and are held in place by a flange that applies uniform pressure to the surface of the disks, ensuring good contact between the individual pieces. The rest of the feed is fabricated from sheet metal disks and bands with the exception of a transition flange and an aperture flange which are machined from cast aluminum. The disks and bands form the flanges and corrugations of the feed. The transition flange and the aperture flange are chromated before assembly. Starting with the aperture flange, the bands and rings are stacked and held in place by hold-down assemblies. Aluminum paint is applied to all ring/band joints. Filler is applied to cover the outside surface of the bands. The assembly is covered on the outside first with tape/epoxy and then with two layers of cloth/resin. A detailed fabrication procedure is given in [4]. Figure 3 shows a longitudinal view of the feed. The feed has an inside diameter of 57.8" at the aperture with an outside diameter of 63.75" and a length of about 155".

Prototype Feed at C-Band:

A prototype of the feed, scaled by a factor of $\frac{1}{4}$, was fabricated to evaluate performance characteristics. The 4-8 GHz frequency range allowed for ease of measurement and, at the same time, kept the size of the feed manageable. The entire scaled feed was machined out of cast aluminum (see Figure 4). An existing circular (diameter 1.93")-to-rectangular (1.872"x0.872") transition was used to measure the prototype feed. Hence, the input diameter of the feed was chosen to be 1.93" instead of 1.875" ($7.5"/4$). Measured and theoretical far-field patterns at 6.0 GHz are shown in Figures 5 and 6. There is excellent match between theory and measurement down to -50 dB. (The outdoor range at Green Bank has a dynamic range of only 50 dB.) The beam is circularly symmetric with good match between the E- and H- plane patterns up to 7.2 GHz. At 7.6 and 8.0 GHz, the measured patterns deviate from theory, indicating the presence of higher order modes. The average taper at 9.3° from 4.0-8.0 GHz is -9.5 dB in the E-plane and -9.8 dB in the H-plane. From 4.8-8.0 GHz, the average tapers in the two planes are -10.5 dB and -10.7 dB. Phase center positions were located by measuring the phase at different longitudinal positions of the feed with respect to the center of rotation until a fairly flat phase plot was obtained. Table 1 shows the phase center distances from the aperture of the horn. The last column gives the phase center distances for the L-band horn obtained from C-band values.

TABLE 1		
Frequency (GHz) C-band (L)	Phase Center Distance From Aperture Plane (inch)	
	C-Band	L-Band
4.0 (1.0)	6.84	26.35
4.4 (1.1)	7.34	28.35
4.8 (1.2)	10.91	42.66
5.2 (1.3)	13.50	52.98
5.6 (1.4)	15.95	62.79
6.0 (1.5)	18.38	72.52
6.4 (1.6)	20.44	80.78
7.2 (1.8)	26.0	102.98
8.0 (2.0)	31.02	123.06

The cross-polarized sidelobes in the 45° plane are below -28 dB for frequencies at and below 7.2 GHz. Figure 7 shows the co-polarized and cross-polarized patterns at 6 GHz in the 45° plane. The peaks of the cross-polarized sidelobes at 7.6 GHz and 8.0 GHz measured -16.5 dB and -5.0 dB, respectively. The oversized (1.872" x 0.872") rectangular waveguide used in the measurements supports higher order modes and is perhaps the reason for the poor cross-polarization performance at the high end of the band. A 1.59" x 0.6" rectangular waveguide-to-coax adapter was mated directly with the 1.872" x 0.872" waveguide and this reduced the cross-polarized sidelobes to -17.5 dB and -17.0 dB at 7.6 GHz and 8.0 GHz, respectively. The measured pattern at 7.6 GHz is shown in Figure 8. Measured return loss of the feed is shown in Figure 9. This measurement was also done with the 1.59"-wide waveguide-to-coax transition. The return loss is -15.7 dB at 4.0 GHz and is -20 dB at 4.1 GHz, corresponding to 1.025 GHz at L-band. The ripple at the high end is partly due to calibration errors and partly due to the presence of higher order modes.

Prototype Feed at L-Band:

A prototype feed was fabricated using sheet metal components and machined parts as described earlier. All parts were fabricated at the VLA machine shop with the exception of the transition flange and the aperture flange. The feed attaches to the feed cone assembly through the transition flange. The assembly was done at the antenna service hanger at the VLA site and the fiberglass application was done at LTC Corporation in Albuquerque, NM. A view of the fabricated feed is shown in Figure 10. To ensure that the fabrication methodology rendered satisfactory electrical performance and resolve some uncertainties with cross-polarized sidelobes and ripples in return loss at the high end of the band, detailed measurements were carried out on the L-band prototype feed. Near-field and far-field radiation patterns of the feed were measured at Composite Optics, Inc. (COI) in San Diego, CA on March 4, 5 and 8, 2004. In order to

suppress higher order modes, the measurement was split into 2 bands: 1.0-1.5 GHz using a 7.70" x 3.85" waveguide, and 1.45-2.0 GHz with a 5.10" x 2.55" waveguide. A circular-to-rectangular (7.5" diameter; 7.70" x 3.85") stepped transition was designed and built for the low frequency band measurement. For the higher band, circular and rectangular waveguide adapters were made to mate with an existing 6.43" diameter circular to 6.5" x 3.25" rectangular transition. Co-polar patterns in the principal planes, as well as in the 45° plane, and cross-polar patterns in the 45° plane were measured. The far-field distance of the feed is about 95' at 2.0 GHz. Measurements were carried out in the parking lot of COI in order to achieve this distance.

Near-Field Measurement:

The feed was placed on a foam cradle and secured by straps. The cradle was set on a foam column which, in turn, was mounted on an azimuth turntable (Figure 11). The feed's center of gravity was roughly on the axis of the foam column. The axis of rotation was 84" behind the aperture plane of the feed. The longitudinal axis of the feed was 12.5 feet above ground level. Near-field patterns were measured first. The distance between the phase center of the transmit horn and the center of rotation was set at 328" for the near-field measurement. This is equivalent to the distance from the feed aperture to the subreflector vertex when the feed is installed on the VLA antenna. Near-field measurements were made to determine if the pattern incident on the subreflector deviated from the far-field pattern. Patterns were measured in two sets, one from 0.95-1.50 GHz and the other from 1.40-2.20 GHz, with the two different transitions. A frequency step of 0.05 GHz was used and the feed was swept from -180° to +180°. Figures 12 and 13 show the E- and H-plane patterns at 1.0 GHz and 1.5 GHz, respectively. The near-field angle correction has been applied in these plots. There is good circular symmetry of the beam. Patterns at other frequencies are also circularly symmetric. The near-field patterns are compared to the far-field patterns in the next section.

Far-Field Measurement:

Far-field measurements were carried out by setting the distance between the source and the antenna under test at about 130 feet. Time-gating was used for measurements at the lower band (0.95-1.50 GHz) to take out reflections longer than about 10 feet over the direct path of 130 feet. A frequency interval of 0.005 GHz was used and, hence, the angle range was limited to -90° to +90° in order to conserve time. Far-field patterns at 1.0 GHz superimposed on near-field patterns are shown in Figures 14 and 15. The two patterns are coincident within the angle subtended by the subreflector ($\pm 9.3^\circ$). The discrepancy at the shoulders is due to the differential phase of the HE_{11} and HE_{12} modes at the two distances. Mismatches at wider angles are due to reflections present in the far-field measurement. Time-gating was not used for the upper band measurements. The frequency interval used was 0.05 GHz and measurements were done for rotation angles of $\pm 180^\circ$. Superimposed far- and near-field patterns at 1.8 GHz are shown in Figures 16 and 17. The increased sidelobes past 45° in the far-field are due to reflections from various sources. Sidelobes in the range +45° to +95° are due to reflections from lamp posts in the parking lot. At angles past about +140°, reflections are from the building that houses the COI facilities. The source of each peak has been identified. On the negative angles, reflections are mainly due to trees and bushes. Figures 18 through 21 show measured far-field patterns superimposed on theoretical patterns at 1.2 GHz and 1.8 GHz. At 1.2 GHz, where time-gating

was used, the patterns follow theory quite well up to $\pm 90^\circ$. At 1.8 GHz, the agreement with theory is good only in the $\pm 20^\circ$ range. Outside this range, reflections in measurements are responsible for the mismatch.

The agreement between measurements and theory is good at other frequencies as well. Figures 22 and 23 show the co-polar and cross-polar measured patterns in the 45° plane at 1.8 GHz and 1.9 GHz, respectively. The 1.9 GHz patterns correspond to the C-band frequency of 7.6 GHz (Figure 8). The peak of the cross-polarized sidelobe at 1.9 GHz is -33 dB, indicating that the high cross-polarized sidelobes measured on the scaled feed were due to overmoding in the waveguide used. Cross-polarization is lower than -27 dB in the entire 1-2 GHz range for the L-band feed. Table 2 gives the measured illumination taper in the E- and H-planes for the L-band feed.

Frequency (GHz)	Taper at 9.3° (dB)	
	E-plane	H-plane
1.0	-5.7	-6.1
1.1	-5.9	-6.8
1.2	-8.0	-8.2
1.3	-11.2	-10.4
1.4	-10.0	-10.6
1.5	-10.4	-10.8
1.6	-11.4	-11.2
1.7	-11.5	-11.0
1.8	-10.0	-10.2
1.9	-10.6	-9.7
2.0	-10.0	-10.6

Return Loss Measurement:

VSWR measurement was carried out on the feed at the VLA site on March 10, 2004 using a vector network analyzer. The feed was suspended from an overhead crane and pointed towards the sky at an elevation angle of about 60° . Two circular waveguide offset shorts and a sliding load were used in the calibration. The measurement was done in two bands and separate calibrations were done for each band using the two different size rectangular waveguide components. The results were combined and are shown in Figure 24. Measurements were taken with and without a radome. The radome material is Escolam 10 with a thickness of 25 mils. When the radome is present, return loss is higher by about 10 dB at frequencies above 1.18 GHz. The ripple frequency corresponds to the round-trip distance from the calibration plane to the feed aperture plane. For either case, return loss is -16 dB at 1.0 GHz and -20 dB at 1.03 GHz. These values agree well with the C-band measurement. The ripple in Figure 9 at the high end of the C-band feed is not present in this case.

Aperture Efficiency and Spillover Temperature:

Using theoretical feed patterns, aperture efficiency of the VLA antenna and spillover temperature were calculated using a software based on Physical Optics technique. Only subreflector blockage was included in these calculations. It was assumed that the phase center at each frequency was at the secondary focus of the telescope. Table 3 lists efficiency and spillover temperatures at four elevation angles. The efficiency varies between 46% and 62%. Calculations were repeated using measured far-field amplitude and phase patterns. These calculations were done only at 1.4 GHz and 2.0 GHz due to the complexity of the computations with the above-mentioned software. With the feed located with its aperture 29" above the secondary focus, the reference point of measurement was 55" below the focus. The subreflector surface was defined with respect to this point, and aperture efficiency was calculated. These results are listed in Table 4 in the "Eff. Before Correction" column. The subreflector position was optimized to maximize the gain, and the translations required at 1.4 GHz and 2.0 GHz are 0.75" and 1.75", respectively, towards the main reflector. The efficiency after phase correction is listed in column 3 of Table 4. A plot of the variation of efficiency as a function of subreflector translation is shown in Figure 25. Rick Perley *et al.* [5] measured aperture efficiency of 0.43 and 0.54 at 1.425 GHz and 1.975 GHz, respectively. Calculated antenna beam patterns are shown in Figures 26 and 27. The half-power beamwidths are 31 and 20 arc minutes at 1.4 and 2.0 GHz, respectively.

Frequency (GHz)	Aperture Eff.	Spillover Temp. (K)			
		90	60	30	20
1.0	0.456	26.3	24.9	28.9	30.4
1.2	0.485	18.0	17.6	19.5	20.3
1.4	0.557	12.7	12.3	14.2	14.9
1.6	0.543	15.6	14.4	15.9	16.3
1.8	0.596	16.2	16.3	17.8	18.0
2.0	0.622	12.2	12.1	13.2	13.5

Frequency (GHz)	Eff. Before Correction	Eff. After Correction
1.4	0.430	0.453
2.0	0.407	0.537

Conclusion:

The illumination taper of the feed at the edge of the subreflector (9.3°) averages to -10.3 dB in the 1.2-2.0 GHz range. The measured pattern on the L-band feed agrees well with theory and with measurements made on the C-band prototype feed. The feed has excellent return loss and low cross-polarized sidelobes. The feed meets the design specifications, and the measurements indicate that the fabrication process works well. The location of the phase center of the feed from the aperture plane, deduced from measurements on the C-band prototype feed, varies between 26.3" to 123" from 1.0 to 2.0 GHz. Calculated aperture efficiency is within $\pm 5\%$ of the measured value.

Acknowledgements:

H. Sipe and D. Barker machined the scaled prototype feed at the Green Bank machine shop. Ramon Gutierrez, Ramon Molina, and Mel Peralta fabricated the sheet metal parts of the feed at the VLA site. Pat Madigan, Garry Morris and Greg Hendley (VLA machine shop) machined parts for the mode converter and the input section of this feed. Components of the circular-to-rectangular transition were machined by Greg Hendley. G. Anderson and J. Bauserman assisted in measurements of the scaled feed at the antenna range in Green Bank. R. Gutierrez at the VLA site transported the L-band feed by truck to San Diego and helped in the measurements. D. Weatherington, W. McNaul and B. Parsons of COI carried out the near-field and far-field measurements on the L-band feed.

References:

- [1] B. K. Watson, A. W. Rudge, R. Dang and A. D. Olver, "Compact Low Cross-Polar Corrugated Feed for E.C.S.," *IEEE Antennas Propagat. Conf. Digest*, Quebec, vol. 1, pp. 209-212, June 1980.
- [2] G. L. James, "Design of Wide-Band Compact Corrugated Horns," *IEEE Trans. Antennas Propagat.*, vol. AP-32, pp. 1134-1138, Oct. 1984.
- [3] Y. Takeichi, T. Hashimoto and F. Takeda, "The Ring-Loaded Corrugated Waveguide," *IEEE Trans. Microwave Theory Tech.*, vol. MTT-19, pp. 947-950, Dec. 1971.
- [4] J. Ruff, "Fiberglass Laminating EVLA C-, S- and L-band Feed Horns," NRAO EVLA Project Specification No. 23665S001, Jan. 4, 2005.
- [5] R. Perley, R. Hayward and D. Mertely, "Testing the EVLA L-Band Feed," NRAO EVLA Memo 85, Nov. 16, 2004.

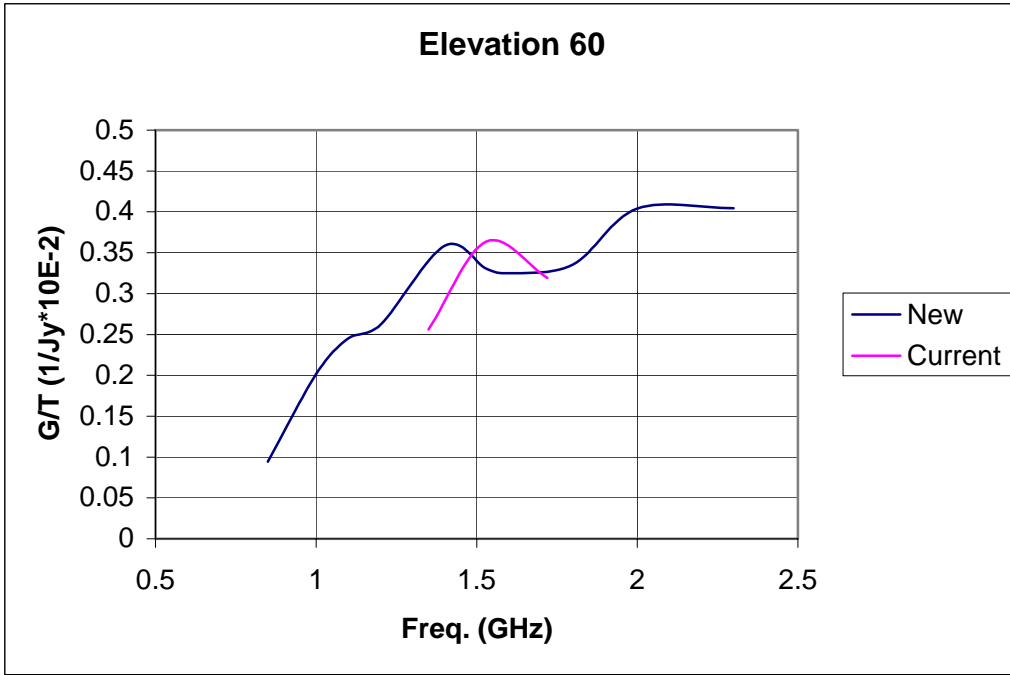


Fig. 1. G/T comparison at 60° elevation.

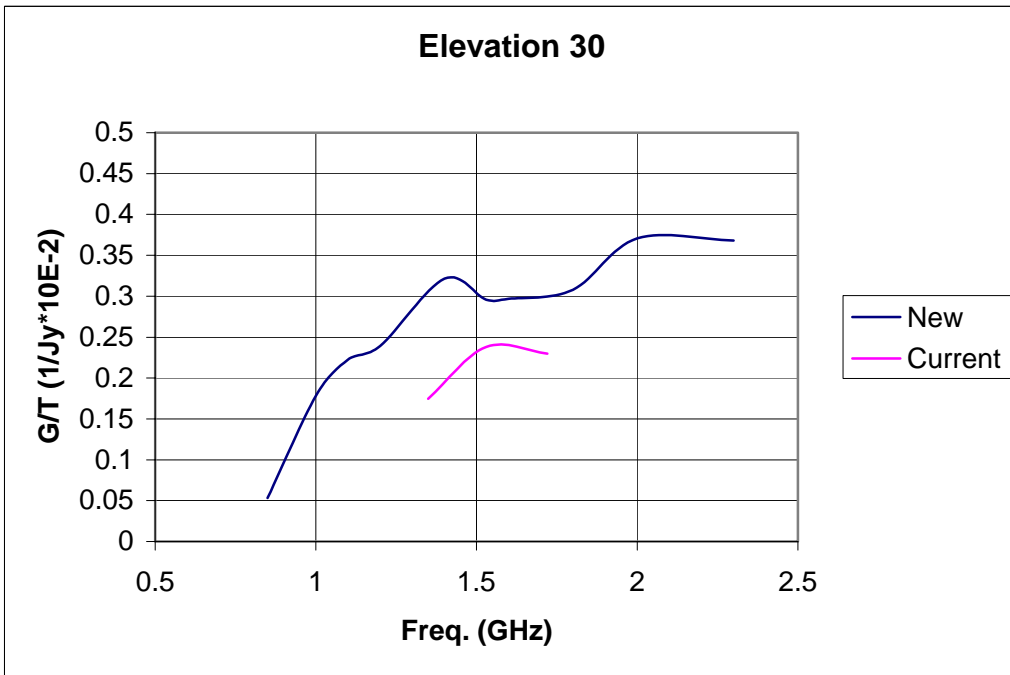


Fig. 2. G/T comparison at 30° elevation.

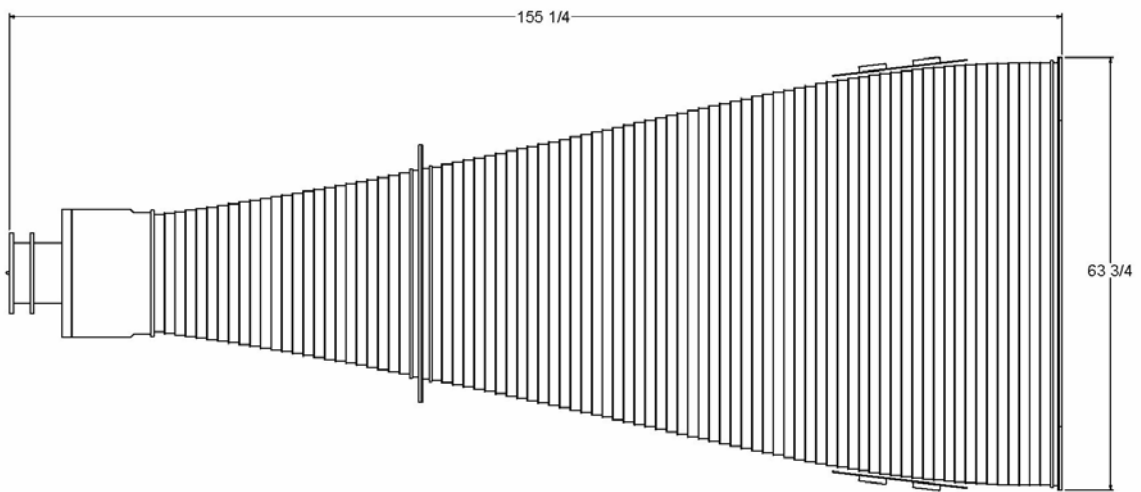


Fig. 3. Longitudinal view of L-band horn.



Fig. 4. Prototype horn at C-band (4-8 GHz).

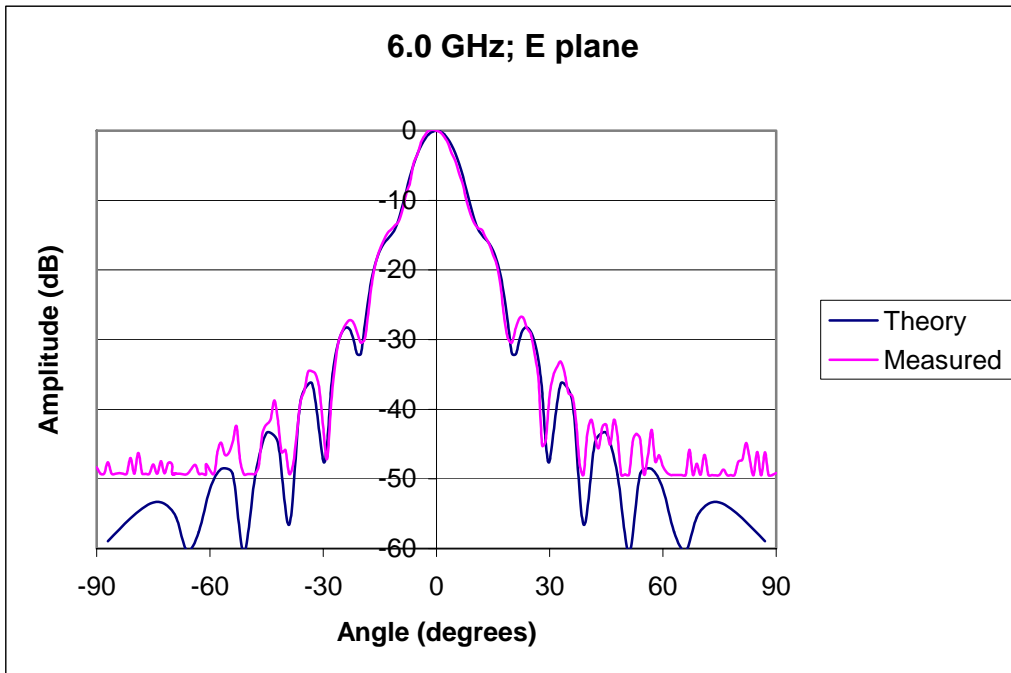


Fig. 5. Far-field pattern of scaled prototype feed at 6.0 GHz, E-plane.

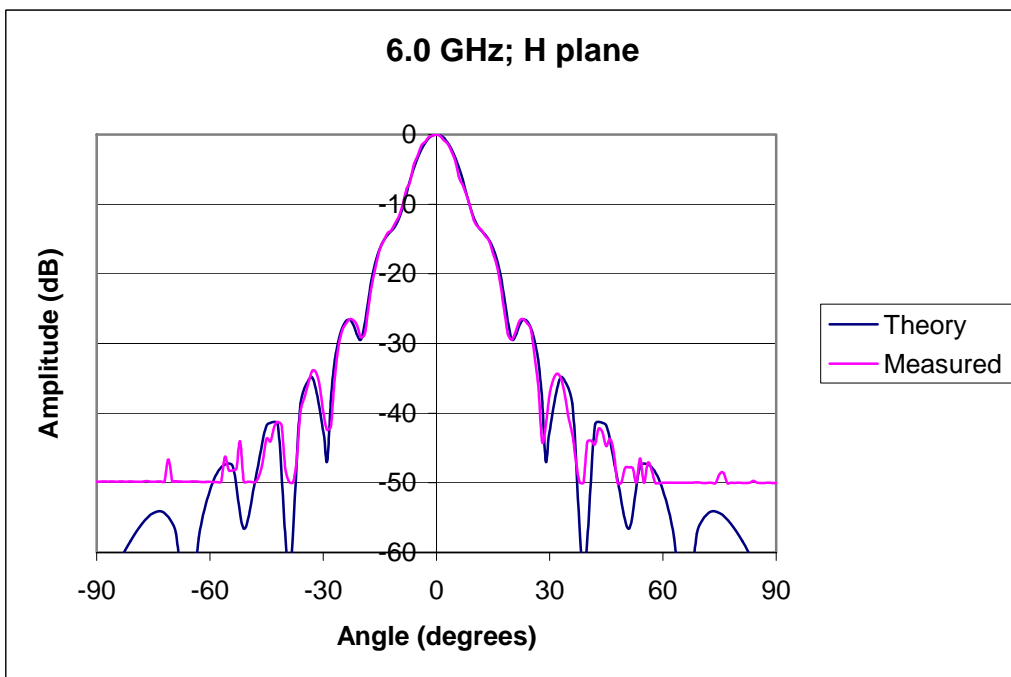


Fig. 6. Far-field pattern of scaled prototype feed at 6.0 GHz, H-plane.

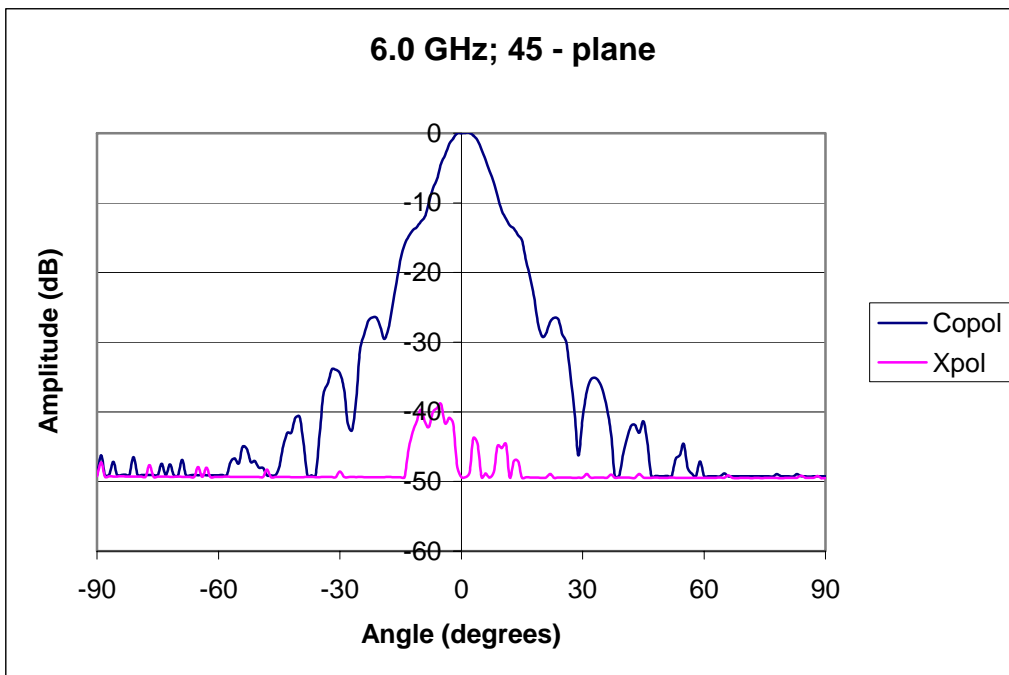


Fig. 7. Measured far-field pattern of scaled prototype feed at 6.0 GHz, 45°-plane.

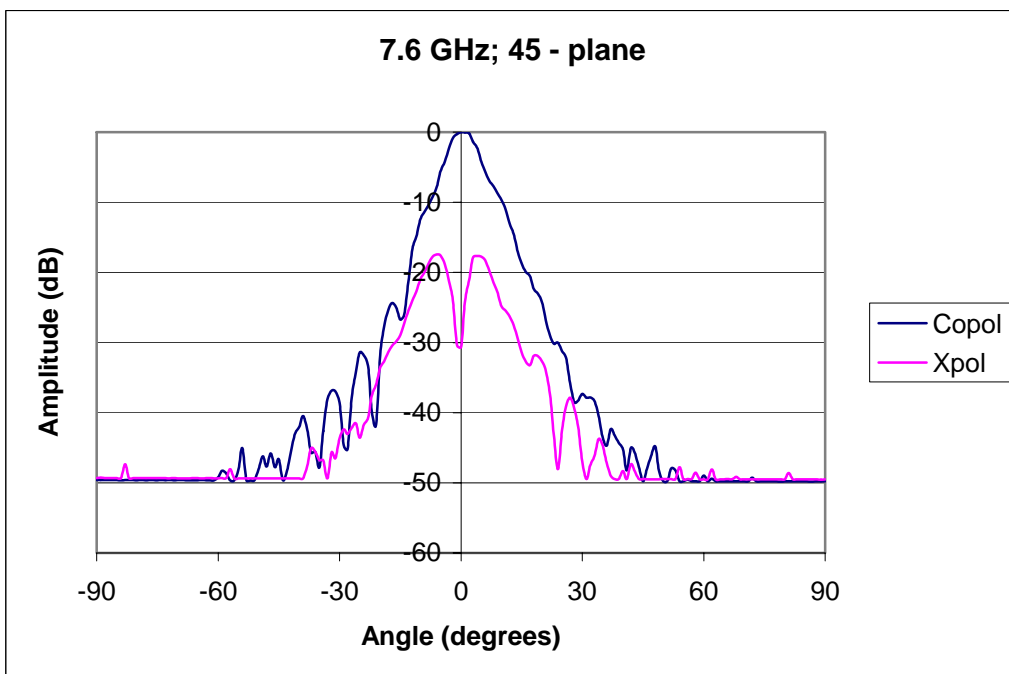


Fig. 8. Measured far-field pattern of scaled prototype feed at 7.6 GHz, 45°-plane.

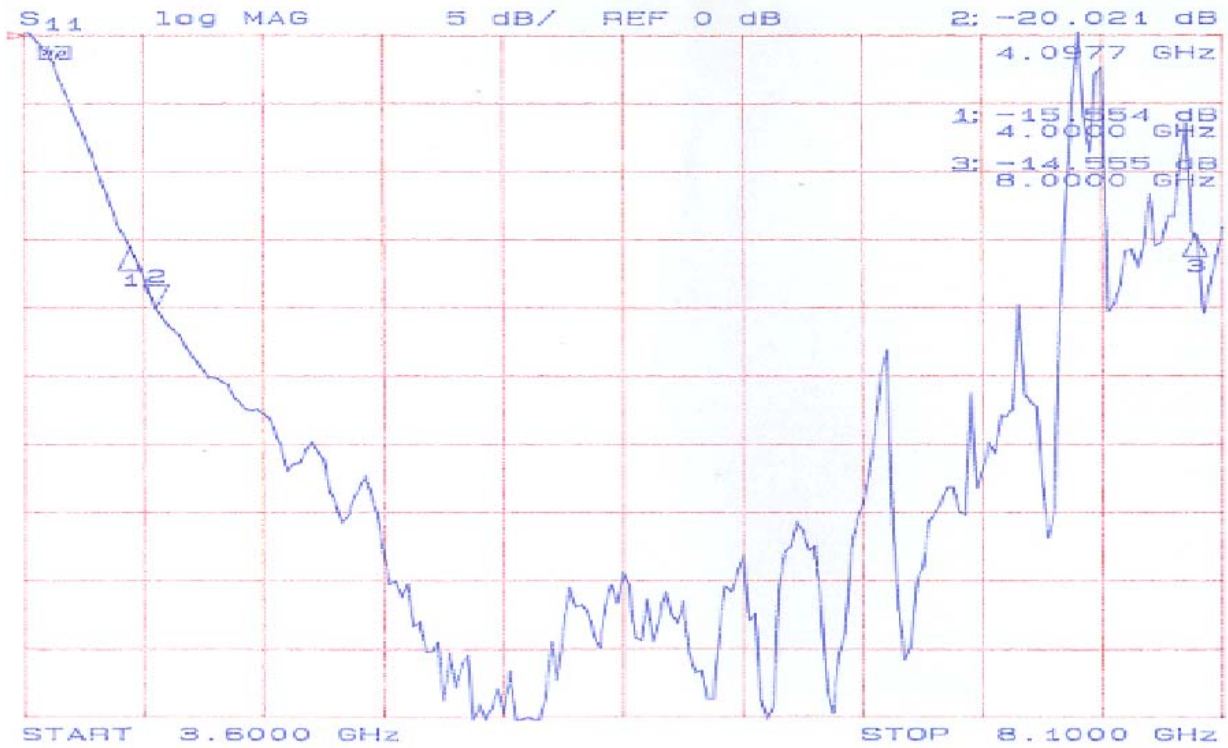


Fig. 9. Measured return loss using 1.59" x 0.60" waveguide.



Fig. 10. L-band feed.



Fig. 11. Feed mounted on azimuth turntable at COI.

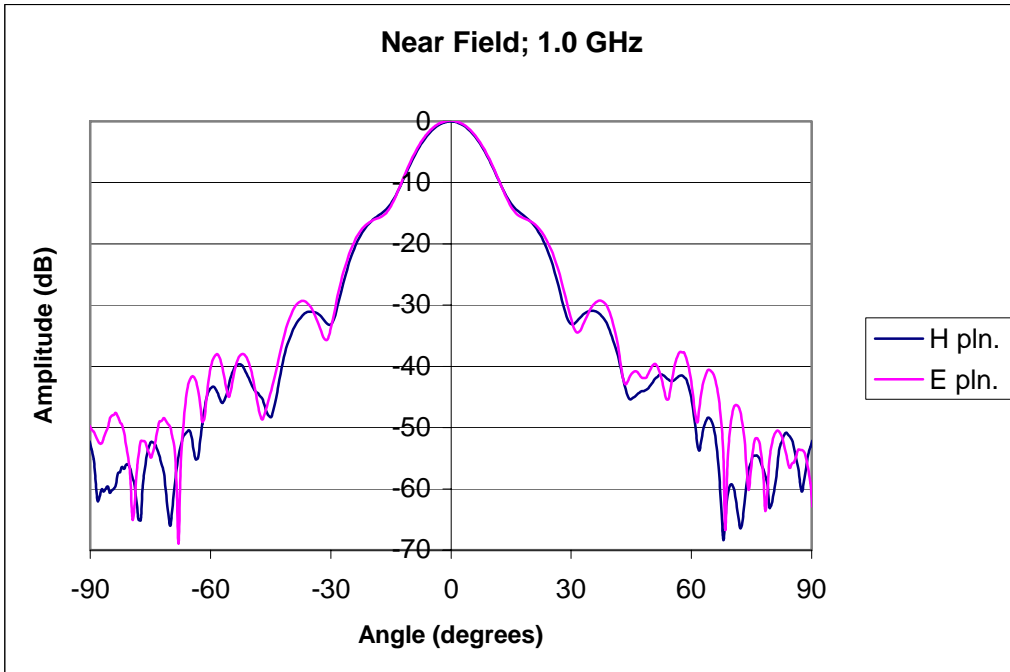


Fig. 12. Measured near-field patterns of L-band feed at 1.0 GHz.

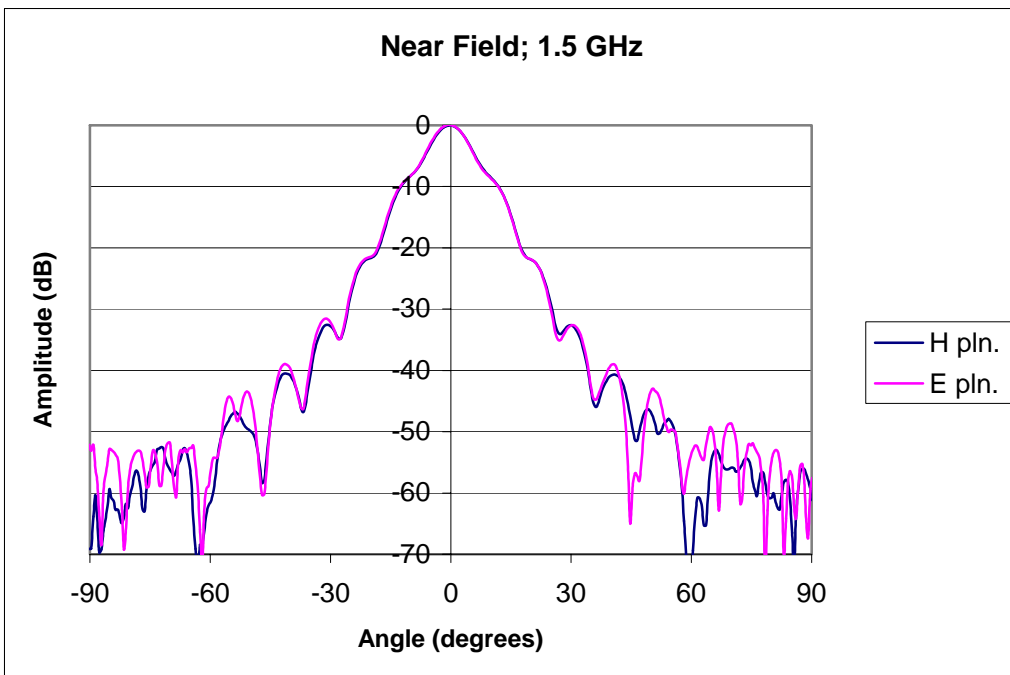


Fig. 13. Measured near-field patterns of L-band feed at 1.5 GHz.

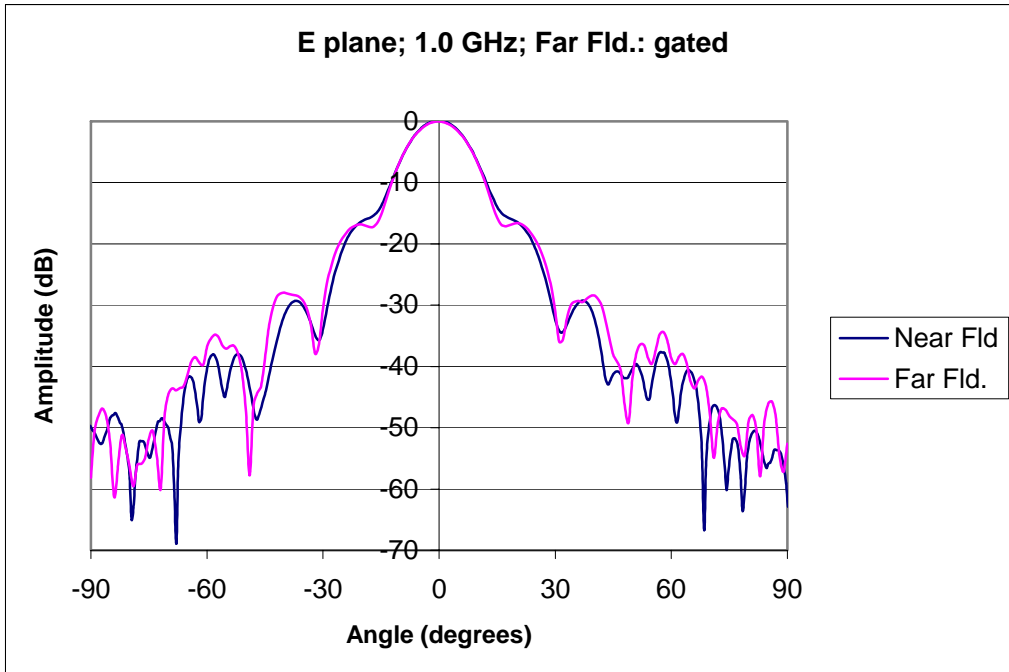


Fig. 14. Measured near- and far-field patterns of L-band feed at 1.0 GHz, E-plane.

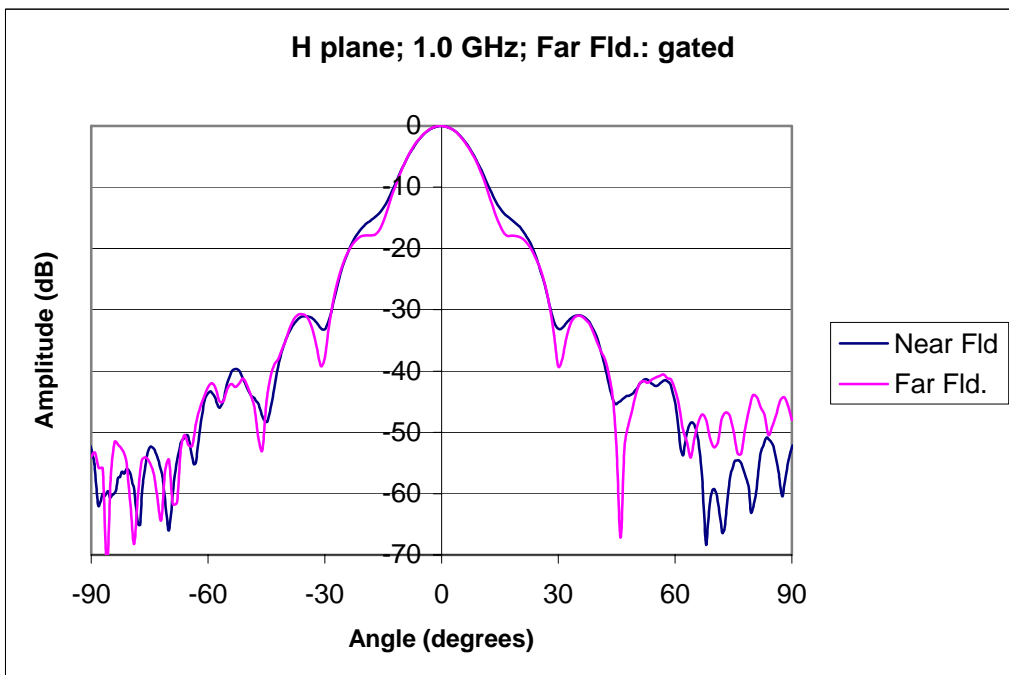


Fig. 15. Measured near- and far-field patterns of L-band feed at 1.0 GHz, H-plane.

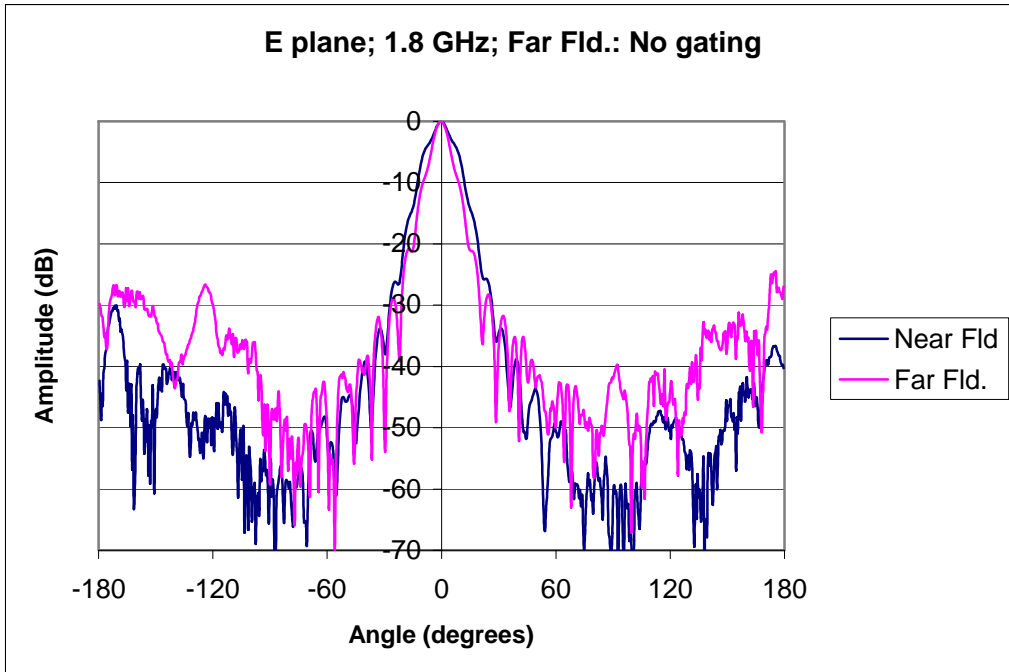


Fig. 16. Measured near- and far-field patterns of L-band feed at 1.8 GHz, E-plane.

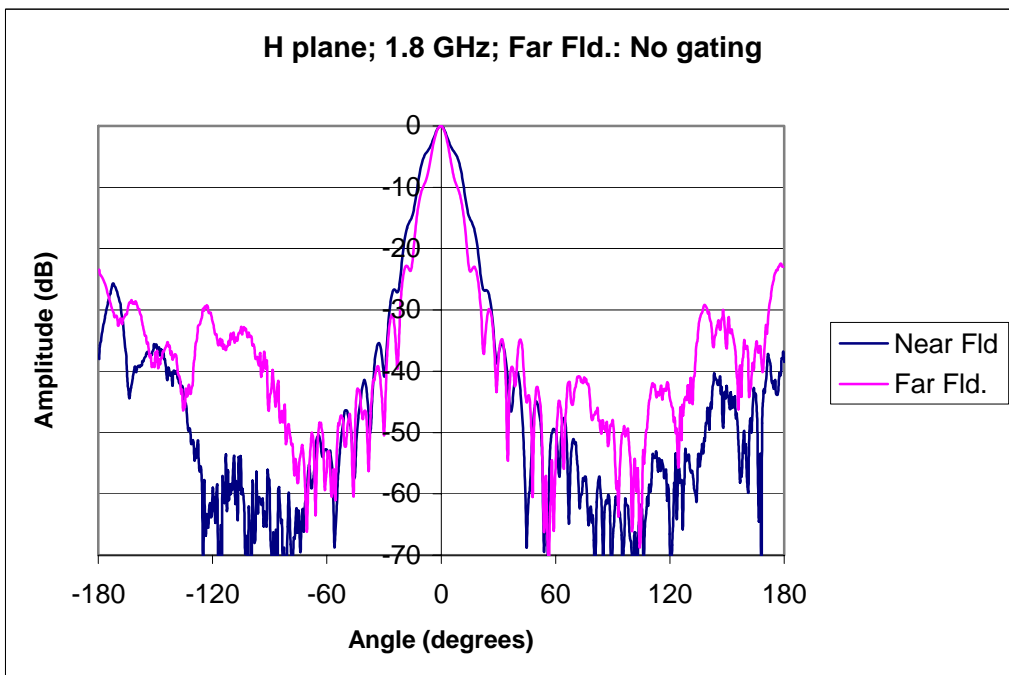


Fig. 17. Measured near- and far-field patterns of L-band feed at 1.8 GHz, H-plane.

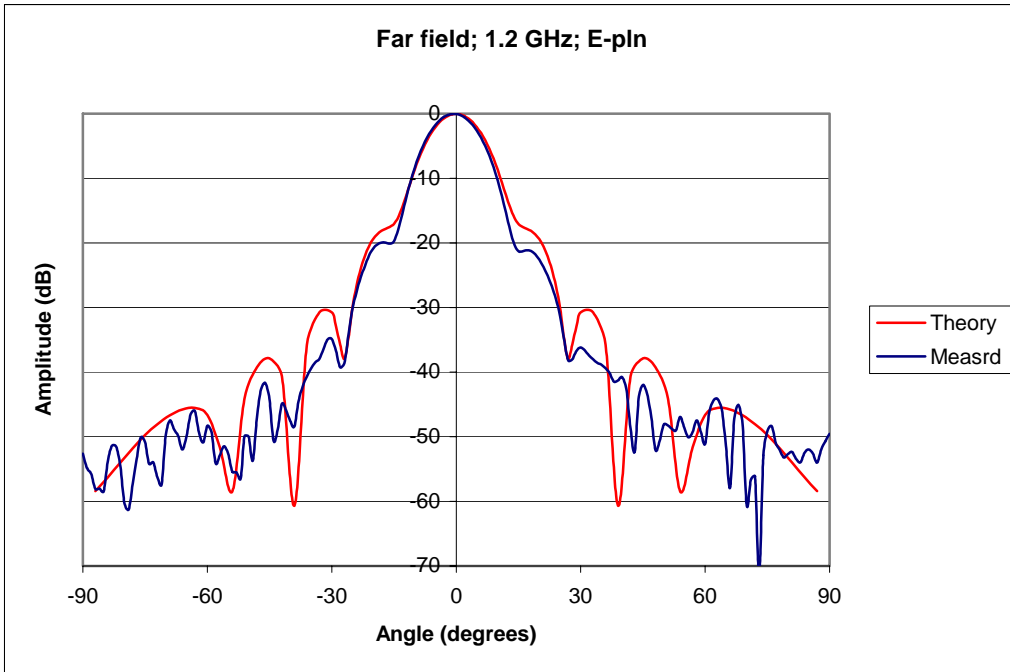


Fig. 18. Far-field pattern of L-band feed at 1.2 GHz, E-plane.

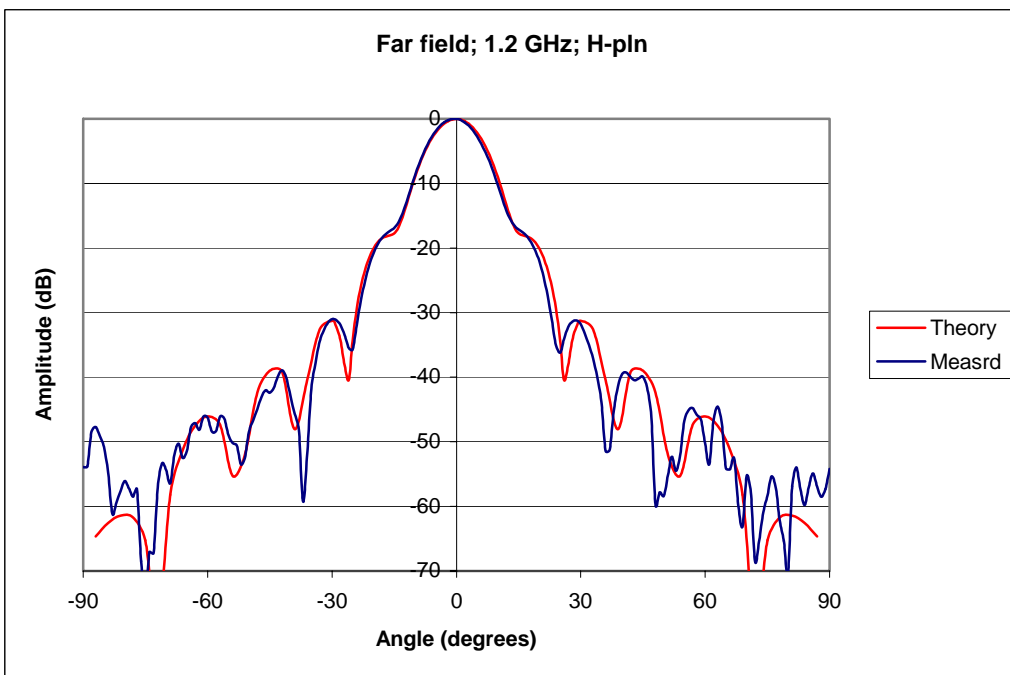


Fig. 19. Far-field pattern of L-band feed at 1.2 GHz, H-plane.

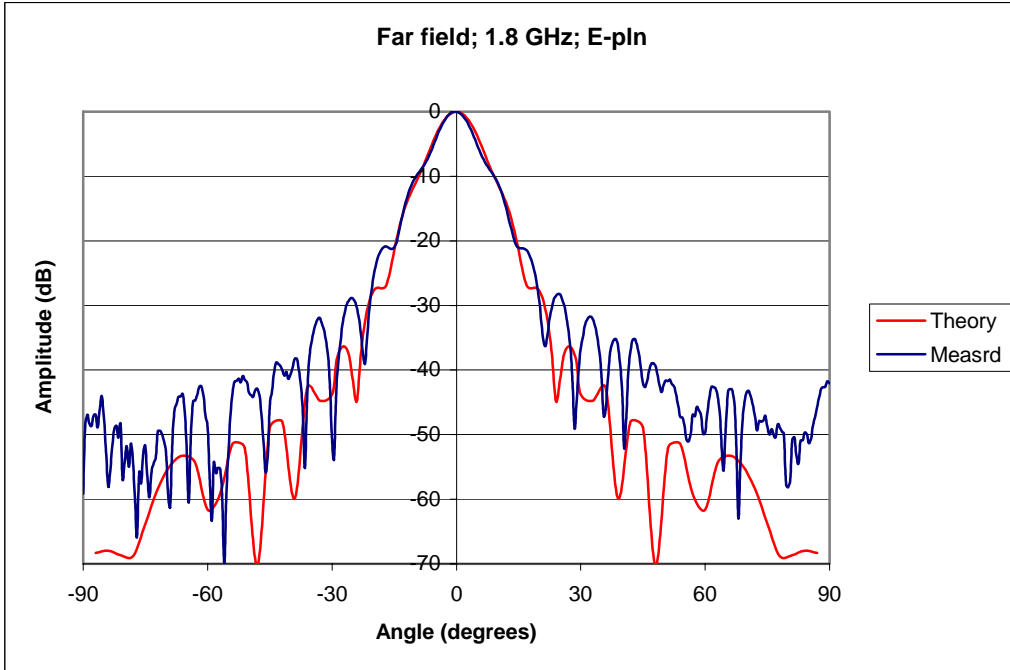


Fig. 20. Far-field pattern of L-band feed at 1.8 GHz, E-plane.

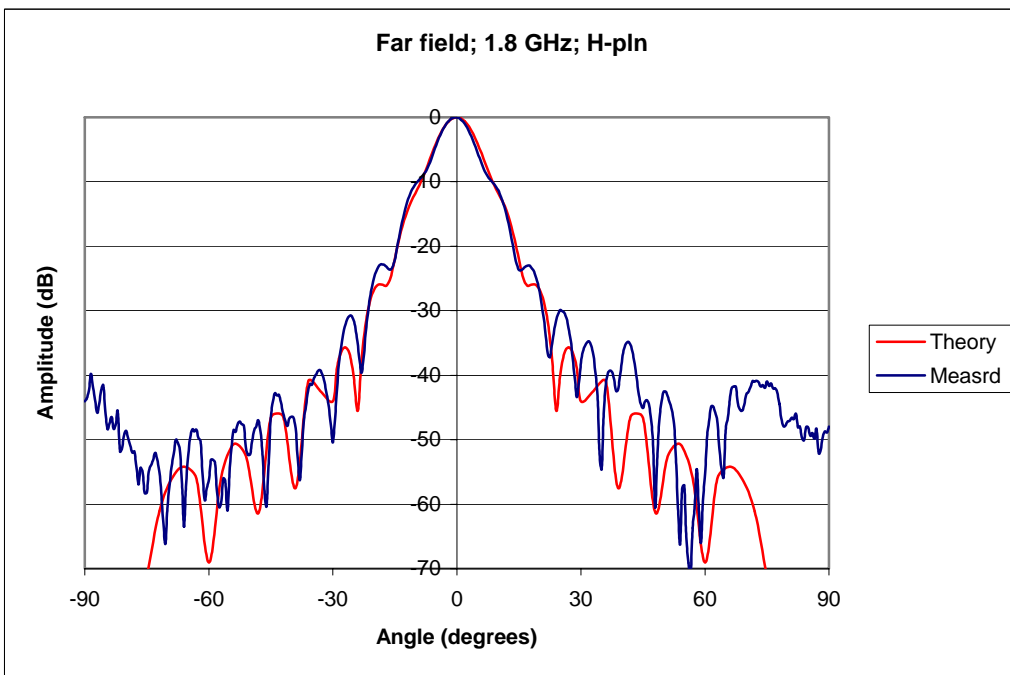


Fig. 21. Far-field pattern of L-band feed at 1.8 GHz, H-plane.

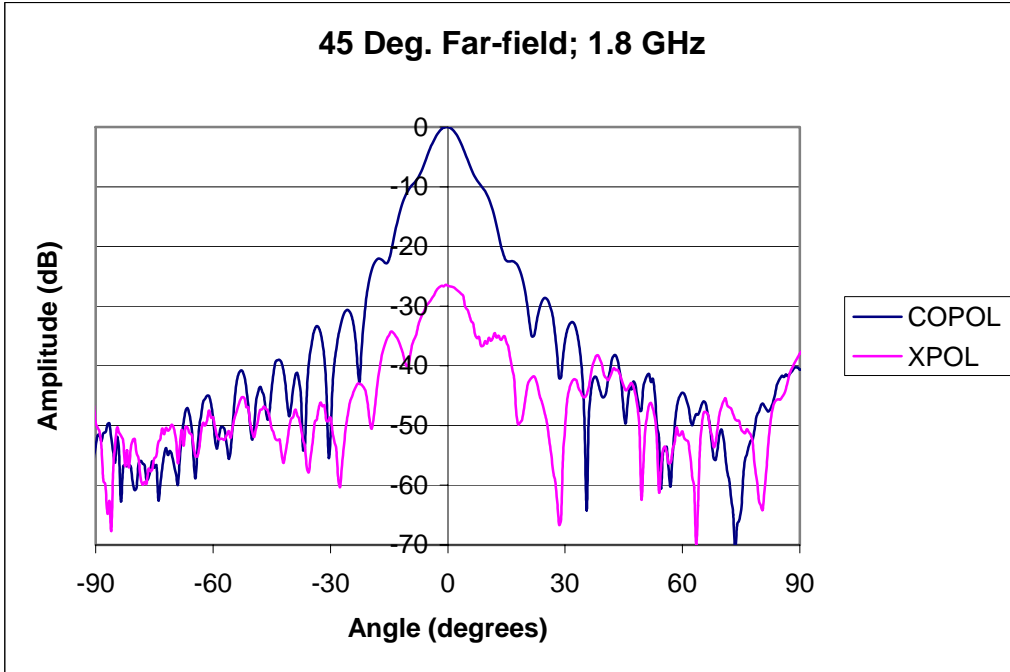


Fig. 22. Co- and cross-polar patterns of L-band feed at 1.8 GHz; 45°-plane.

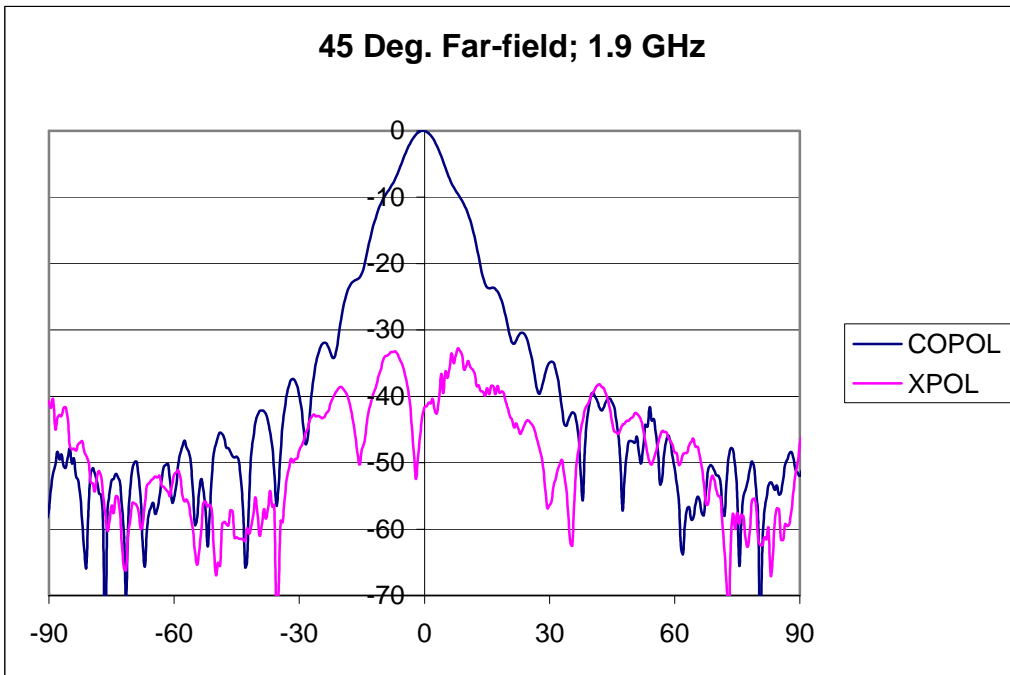


Fig. 23. Co- and cross-polar patterns of L-band feed at 1.9 GHz; 45°-plane.

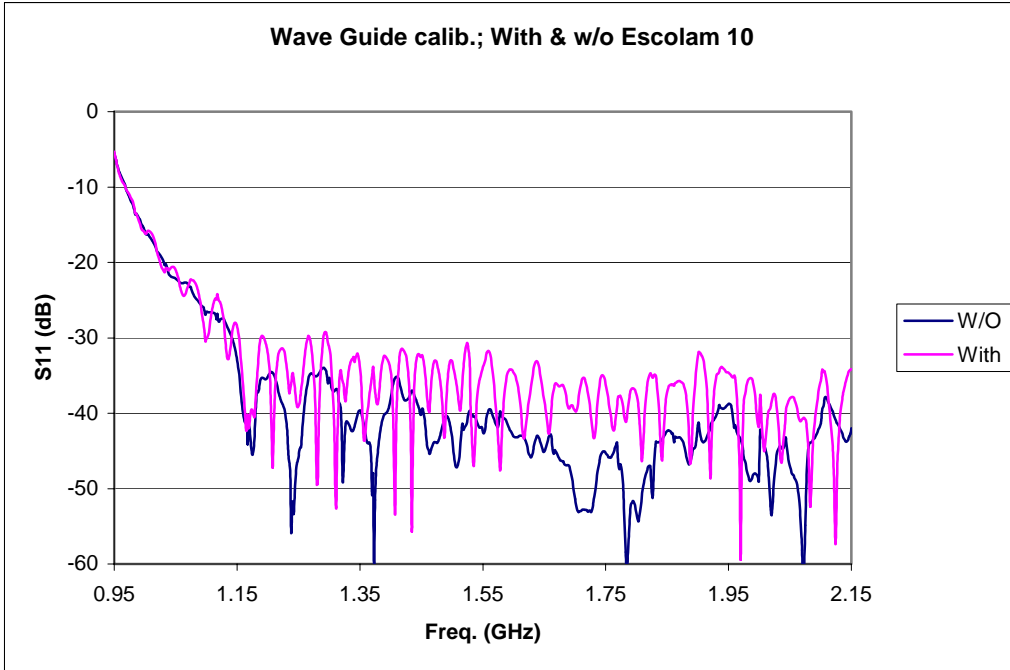


Fig. 24. Measured return loss of L-band feed with and without radome.

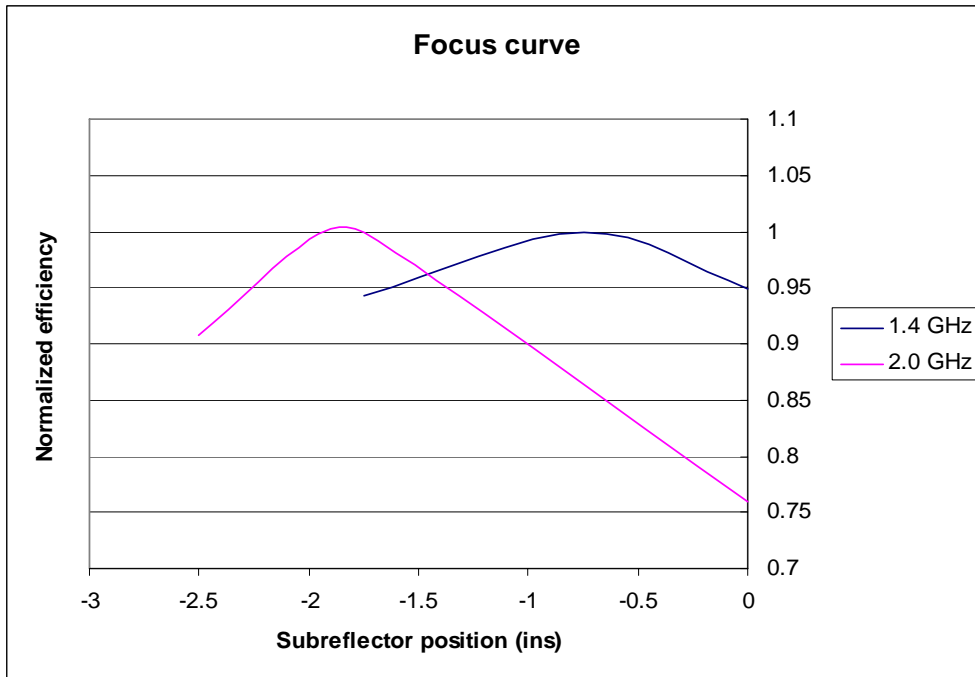


Fig. 25. Normalized efficiency as a function of subreflector translation. Negative numbers indicate translation towards the main reflector from nominal position.

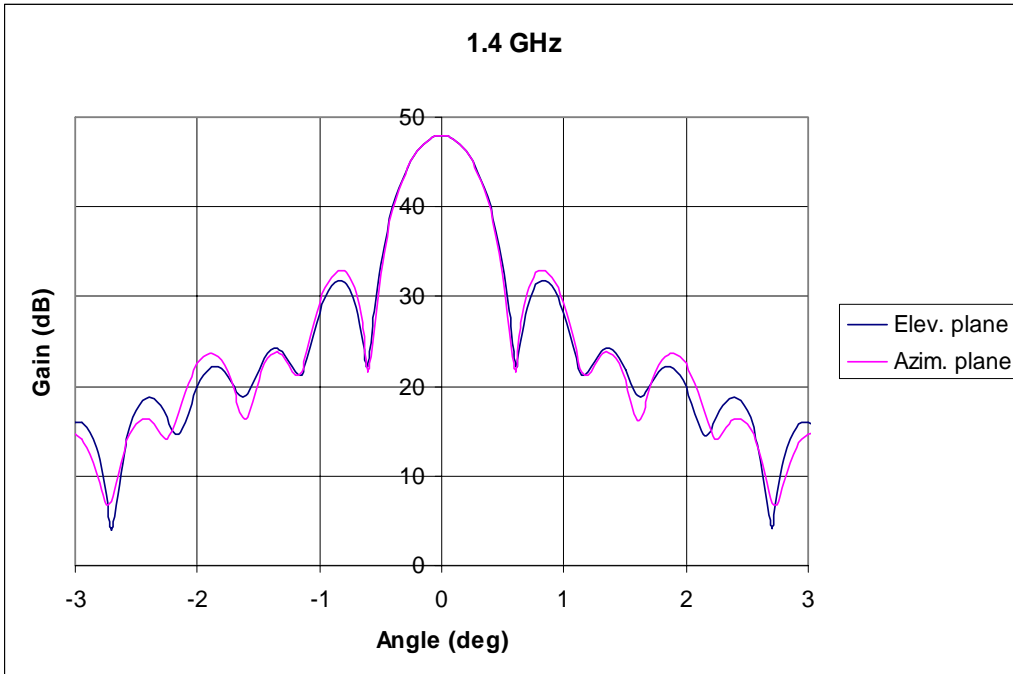


Fig. 26. Beam of the antenna at 1.4 GHz.

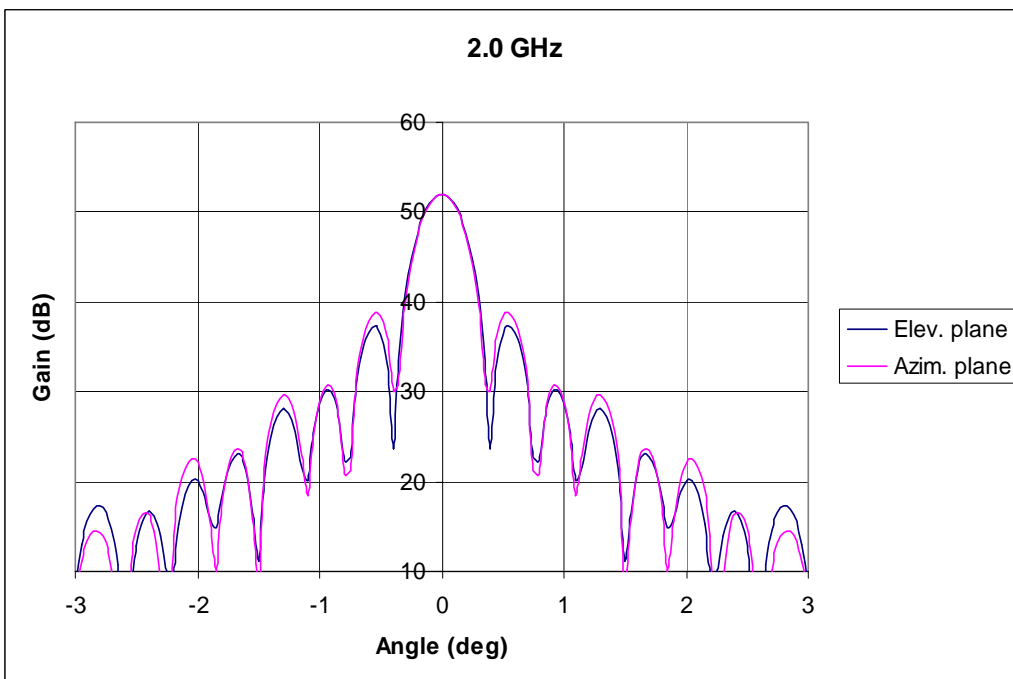


Fig. 27. Beam of the antenna at 2.0 GHz.